

---

# Object Files and Schemata: Factorizing Declarative and Procedural Knowledge in Dynamical Systems

---

Anirudh Goyal<sup>1</sup>, Alex Lamb<sup>1</sup>, Phanideep Gampa<sup>1,2</sup>, Philippe Beaudoin<sup>3</sup>, Sergey Levine<sup>4</sup>, Charles Blundell<sup>5</sup>, Yoshua Bengio<sup>1</sup>, Michael Mozer<sup>6</sup>

## Abstract

Modeling a structured, dynamic environment like a video game requires keeping track of the objects and their states (*declarative* knowledge) as well as predicting how objects behave (*procedural* knowledge). Black-box models with a monolithic hidden state often lack *systematicity*: they fail to apply procedural knowledge consistently and uniformly. For example, in a video game, correct prediction of one enemy’s trajectory does not ensure correct prediction of another’s. We address this issue via an architecture that factorizes declarative and procedural knowledge and that imposes modularity within each form of knowledge. The architecture consists of active modules called *object files* that maintain the state of a single object and invoke passive external knowledge sources called *schemata* that prescribe state updates. To use a video game as an illustration, two enemies of the same type will share schemata but will each have their own object file to encode their distinct state (e.g., health, position). We propose to use attention to control the determination of which object files to update, the selection of schemata, and the propagation of information between object files. The resulting architecture is a drop-in replacement conforming to the same input-output interface as normal recurrent networks (e.g., LSTM, GRU) yet achieves substantially better generalization on environments that have factorized declarative and procedural knowledge, including a challenging intuitive physics benchmark.

## 1 Introduction

An intelligent agent that interacts with its world must not only perceive objects but must also remember its past history and experience with these objects. The wicker chair in one’s living room is not just a chair, it is the chair which has an unsteady leg and easily tips. Your keys may not be visible, but you remember placing them on the ledge by the door. Even more trivially, the fly buzzing in your left ear is the same fly you saw earlier which landed on the table.

Visual cognition requires a short-term memory that keeps track of object locations, trajectories, and other properties. In the cognitive science literature, this particular form of memory is often referred to as an *object file* [Kahneman et al., 1992]. An object file is characterized by a representation that acts as a temporally persistent reference to an external object, permitting a sort of object constancy or permanence as the object and the viewer move in the world. Each object file stores information concerning the properties and state of an object.

To interpret a complex visual scene, multiple object files must be maintained in parallel. Consider scenes like a pacman video-game screen, people interacting in a public square or on a sports field, or balls rolling and colliding on a pool table. In each of these situations, multiple object *tokens* of the

---

<sup>01</sup> Mila, University of Montreal, <sup>2</sup> IIT BHU, Varanasi, <sup>3</sup> ElementAI, <sup>4</sup> UC Berkeley, <sup>5</sup> Deepmind, <sup>6</sup> Google Research, Brain Team, Corresponding author: anirudhgoyal19119@gmail.com

Object Files	Schema 1 Pacman	Schema 2 Normal Ghost	Schema 3 Scared Ghost
Top Frame			
A	✓		
B		✓	
C		✓	
D		✓	
E		✓	
Bottom Frame			
A	✓		
B			✓
C			✓
D			✓
E			✓

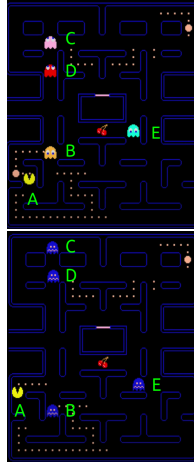


Figure 1: As a motivating example, we show two successive frames of the game PacMan and show how procedural and declarative knowledge must be dynamically factorized. The “B” ghost has a persistent object file (with its location and velocity), yet its procedure mostly depends on whether it is in its *scared* or *normal* routine.

same *type* are present, and tokens have similar dynamical properties. For example, balls on the pool table operate according to the laws of physics.

We propose a method of separately representing knowledge about the state of a particular object token—the information that is maintained in an object file—and abstract knowledge about the dynamics of the object type. We refer to this latter type of knowledge as a *schema* (plural *schemata*), a term which in the cognitive science literature means a framework for organizing complex knowledge. Here, we specifically use schema to refer to procedural knowledge—knowledge about the dynamics of state evolution—in contrast to the declarative knowledge in an object frame that describes the states themselves (Figure 1). The combination of files and schemata is sufficient to predict future states of visual environments, critical for planning and goal-seeking behavior. For the sake of simplifying terminology, we will refer to object files as ‘files’.

Object-oriented programming (OOP) provides a way to think about the relationship between files and schemata. In OOP, each *object* is an instantiation of an object class and it has a self-contained collection of variables whose values are specific to that object and *methods* that operate on all instances of the same class. The relation between objects and methods mirrors the relationship between our files and schemata. In both OOP and our view of visual cognition, a key principle is the *encapsulation* of knowledge: internal details of objects (files) are hidden from other objects, and methods (schemata) are accessible to all and only objects to which they are applicable.

The modularity of knowledge in OOP supports human programmers in writing code that is readily debugged, extended, and reused. We conjecture that the corresponding modularity of files and schemata will lead to neural network models with more efficient learning and more robust representations.

Modularity is the guiding principle of the model we propose, which we call SCOFF, an acronym for *schema / object-file factorization*. Like other neural net models with external memory [e.g., Mozer and Das, 1993, Graves et al., 2016, Sukhbaatar et al., 2015], SCOFF includes a set of slots which are each designed to contain a file (Figure 2). In contrast to most previous external memory models, the slots are not passive contents waiting to be read or written by an active process, but are dynamic, modular elements that seek information in the environment that is relevant to the object they represent, and when critical information is observed, they update their states, possibly via information provided by other files. Event-based OOP is a good metaphor for this, where external events can trigger the action of objects.

As Figure 2 suggests, there is a factorization of declarative knowledge—the properties and history of an object, as contained in the files—and procedural knowledge—the way that object behave, as contained in the schemata. Whereas declarative knowledge can change rapidly, procedural knowledge is more stable over time. This factorization allows any schema to be applied to any file, when the file deems it appropriate. The model design ensures *systematicity* in the operation of a schema, regardless of the slot to which a file is assigned. Similarly, a file can access any applicable schema regardless of which slot it sits in. Furthermore, a schema can be applied to multiple files at once, and multiple schemata could be applied to a file (e.g., Figure 1). In OOP, systematicity is similarly achieved by

virtue of the fact that the same method can be applied to any object instantiation and that multiple methods exist which can be applied to an object of the appropriate type.

Our key contribution is to demonstrate the feasibility and benefit of factorizing declarative knowledge (the properties and history of an object) and procedural knowledge (the way objects behave). This factorization enforces not only an important form of systematicity, but also of exchangeability: the model behaves exactly the same regardless of the assignment of schemata to schemata-slots and the assignment of objects to file-slots. With this factorization, we find improved accuracy of next-state prediction models and improved interpretability of learned parameters.

## 2 The schemata / object-file factorization (SCOFF) model

SCOFF (Figure 2) is an architectural backbone that supports the separation of procedural and declarative knowledge about dynamical entities (objects) in an input sequence. The input sequence  $\{\mathbf{x}_1, \dots, \mathbf{x}_t, \dots, \mathbf{x}_T\}$ , indexed by time step  $t$  is processed by a CNN to obtain a deep embedding,  $\{\mathbf{z}_1, \dots, \mathbf{z}_t, \dots, \mathbf{z}_T\}$ , which then serves as input to a network with  $n_f$  files and  $n_s$  schemata.

Files are active processing components that maintain and update their internal state. Essentially, a file is a layer of GRU or LSTM units with three additional bits of machinery, which we now describe.

1. Our earlier metaphor identifying files in SCOFF with objects in OOP is apropos in the sense that files are *event driven*. The file operates in a temporal loop that continuously awaits relevant signals in the input. Relevance is determined by the file’s current state, and its determination is based on a special case of a key-value attention mechanism, which we describe in detail below. When a file is triggered by an input, the file updates by deciding which schema to apply. When it is not triggered, its state remains unchanged for the next time step. (The triggering mechanism is thus distinct from input gating in a GRU [Chung et al., 2014] or LSTM unit: it is all-or-none, and it operates holistically on all units in the layer.) At most  $n_{sel}$  files can thus be activated at each time step, based on a competition between files. The competition is necessary to ensure differentiation of the files during training, as we will demonstrate shortly.
2. Triggering causes a file to perform a one-step update of its state layer of GRU or LSTM units, conditioned on the input signal received. The weight parameters needed to perform this update, which we will denote generically as  $\theta$ , are not—as in a standard GRU or LSTM—internal to the layer but rather are provided externally. Each schema  $j$  is nothing more than a set of parameters  $\theta_j$  which can be plugged into this layer. SCOFF uses a key-value attention mechanism to perform soft selection of the appropriate schema (parameters).
3. Triggered files may also seek information from other files, again using a key-value attention mechanism to query each other file, matching its query to keys provided by each other file, and soft selecting the best matching files to incorporate the values provided by the corresponding files.

This operation cycle ensures that files can update their state in response to both external input and the internal state comprised of all the files contents. This updating is an extra wrapper around the

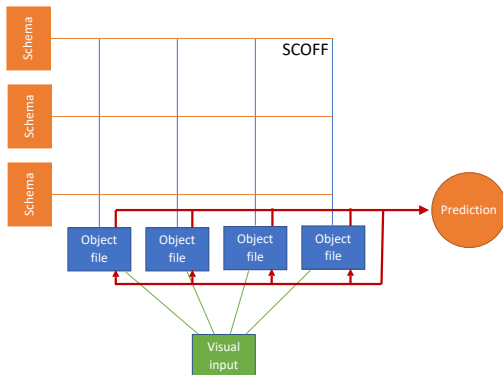


Figure 2: Our SCOFF model. Schemata are sets of parameters that specify the dynamics of objects. Object files are active modules that maintain the time-varying state of an object, seek information from the input, and select schemata for updating.

---

**Algorithm 1** SCOFF model

---

**Input:** Current sequence element,  $\mathbf{x}_t$  and previous file state,  $\{\mathbf{h}_{t-1,k} \mid k \in \{1, \dots, n_f\}\}$

**Step 1: Process image to obtain deep embedding**

- $\mathbf{z}_t = \text{CNN}(\mathbf{x}_t)$

**Step 2: Files compete to read from the input and update their state**

- $\mathbf{q}_k = \mathbf{h}_{t-1,k} \mathbf{W}^q$
- $s_k = \text{logistic}\left(\frac{\mathbf{q}_k \boldsymbol{\kappa}_t}{\sqrt{d_e}}\right)$ , where  $\boldsymbol{\kappa}_t = (\mathbf{z}_t \mathbf{W}^e)^\top$
- Construct a set  $\mathcal{F}_t$  which contains the indices of the  $n_{\text{sel}}$  object files that have the largest  $s_k$
- $\mathbf{a}_k = s_k \mathbf{z}_t \mathbf{W}^v \quad \forall k \in \mathcal{F}_t$

**Step 3: Selected object files pick the most relevant schema and update**

- $\tilde{\mathbf{h}}_{t,k,j} = \text{GRU}_{\boldsymbol{\theta}_j}(\mathbf{a}_k, \mathbf{h}_{t-1,k}) \quad \forall k \in \mathcal{F}_t, j \in \{1, \dots, n_s\}$
- $\tilde{\mathbf{q}}_k = \mathbf{h}_{t-1,k} \tilde{\mathbf{W}}^q$
- $i_k = \text{argmax}_j (\tilde{\mathbf{q}}_k \tilde{\boldsymbol{\kappa}}_{k,j} + \gamma)$ , where  $\tilde{\boldsymbol{\kappa}}_{k,j} = (\tilde{\mathbf{h}}_{t,k,j} \tilde{\mathbf{W}}^e)^\top$  and  $\gamma \sim \text{Gumbel}(0, 1)$
- $\mathbf{h}_{t,k} = \begin{cases} \tilde{\mathbf{h}}_{t,k,i_k} & \forall k \in \mathcal{F}_t \\ \mathbf{h}_{t-1,k} & \text{otherwise} \end{cases}$

**Step 4: Selected object files seek information from other object files**

- $\hat{\mathbf{q}}_k = \mathbf{h}_{t-1,k} \hat{\mathbf{W}}^q \quad \forall k \in \mathcal{F}_t$
  - $s_{k,k'} = \text{softmax}\left(\frac{\hat{\mathbf{q}}_k \hat{\boldsymbol{\kappa}}_{k'}}{\sqrt{d_e}}\right)$  where  $\hat{\boldsymbol{\kappa}}_{k'} = (\mathbf{h}_{t,k'} \hat{\mathbf{W}}^e)^\top \quad \forall k \in \mathcal{F}_t, k' \in \{1, \dots, n_f\}$
  - $\mathbf{h}_{t,k} \leftarrow \mathbf{h}_{t,k} + \sum_{k'} s_{k,k'} \hat{\mathbf{v}}_{k'}$  where  $\hat{\mathbf{v}}_{k'} = \mathbf{h}_{t,k'} \hat{\mathbf{W}}^v \quad \forall k \in \mathcal{F}_t$
- 

ordinary update that takes place in a GRU or LSTM layer. It provides additional flexibility in that (1) files may simply remain dormant and fully ignore an input, (2) files can switch their dynamics from one input to the next conditioned on their internal state, (3) files are modular in that they do not communicate with one another except via state-dependent selective message passing.

Files are placeholders in that a particular file has no parameter specific to that file. Instead, the parameters are provided from two sources: either the schemata or a pool of generic parameters shared by the  $n_f$  files. This generic parameter pool is used to implement key-value attention over the input, the schemata, and communication among files. The sharing of schemata ensures systematicity; the sharing of the generic parameter pool ensures *exchangeability*—model behavior is unaffected by the assignment of object instances to file slots.

## 2.1 SCOFF specifics

Algorithm 1 provides a precise specification of SCOFF broken into four steps. Step 1 is external to SCOFF and involves processing an input to obtain a deep embedding. In the current work our examples are all image sequences, so the processing is performed by a convolutional neural net (CNN). The core steps that follow are as follows.

**Step 2: Files compete to read from the input and update their state.** At time  $t$ , exactly  $n_{\text{sel}}$  files are selected via an attention mechanism as follows. File  $k$  uses its state,  $\mathbf{h}_{t-1,k}$  to form a query,  $\mathbf{q}_k$ , to the current input contents,  $\boldsymbol{\kappa}_t$ , and obtains a goodness of match score ( $s_k$ ). The  $n_{\text{sel}}$  highest scores are selected, forming the set of files  $\mathcal{F}_t$ . A value (in the key-value attention sense),  $\mathbf{a}_k$ , is extracted from the input for each file  $k$  in  $\mathcal{F}_t$ .

**Step 3: Selected files pick the most relevant schema and update.** Each file  $k$  in  $\mathcal{F}_t$  picks one schema via attention as follows. File  $k$  binds to *each* schema  $j$ , and then performs a hypothetical update, yielding  $\tilde{\mathbf{h}}_{t,k,j}$ . In simulations below, the file state is maintained by a GRU layer, and schema  $j$  is a parameterization of the GRU, denoted  $\text{GRU}_{\boldsymbol{\theta}_j}$ , which determines the update. The previous state of the file,  $\mathbf{h}_{t-1,k}$  serves as a query in key-value attention against a key derived from the hypothetical updated state,  $\tilde{\mathbf{h}}_{t,k,j}$ . The schema  $i_k$  corresponding to the best query-key match for file  $k$  is used to update file  $k$ 's state. To facilitate learning, selection is based on the Gumbel-softmax method of stochastic selection [Jang et al., 2016].

**Step 4: Selected files seek information from other files.** This step allows for interactions among files. Each selected file  $k$  queries other files for information relevant to its update as follows. The file’s previous state,  $\mathbf{h}_{t-1,k}$ , is used to form a query,  $\widehat{\mathbf{q}}_k$ , in an attention mechanism against a key derived from the new state of each other file  $k'$ ,  $\widehat{\mathbf{k}}_{k'}$ , and softmax selection ( $s_{k,k'}$ ) is used to integrate information from other files,  $\widehat{\mathbf{v}}'_k$ , into file  $k$ ’s state.

The majority of SCOFF parameters are the schemata,  $\{\boldsymbol{\theta}_j | j \in \{1, \dots, n_s\}\}$ . The remaining parameters are those of query functions ( $\mathbf{W}^q, \widetilde{\mathbf{W}}^q, \widehat{\mathbf{W}}^q$ ), key functions ( $\mathbf{W}^e, \widetilde{\mathbf{W}}^e, \widehat{\mathbf{W}}^e$ ), and value functions ( $\mathbf{W}^v, \widehat{\mathbf{W}}^v$ ). Note that these linear models could be replaced by nonlinear functions. For training, competition among the files to become selected was found important in order for objects to learn to be differentiated.

### 3 Related Work

**CNNs.** SCOFF applies the same knowledge (schemata) to multiple objects (files), yielding systematicity. Similarly, a CNN is a highly restrictive instantiation of this same notion, where knowledge—in the form of a convolutional filter—is applied uniformly to every location in an image, yielding equivariance. SCOFF is a more flexible architecture than a CNN in that files are defined by abstract notion of objects not a physical patch of an image, and schemata are applied dynamically and flexibly over time, not in a fixed, rigid manner as the filters in a CNN.

**Memory Networks.** A variety of existing models leverage an external slot-based, content-addressable memory [e.g., Graves et al., 2016, Sukhbaatar et al., 2015]. The memory slots are passive elements that are processed by a differentiable neural controller such as an LSTM. Whereas traditional memory networks have many dumb memory cells and one smart controller, SCOFF has many smart memory cells—the files—which also act as local controllers. However, SCOFF shares the notion with memory networks that the same knowledge is applied systematically to every cell.

**Recurrent Entity Networks.** Henaff et al. [2016] describe a collection of recurrent modules that update independently and in parallel in response to each input in a sequence. The module outputs are integrated to form a response. It shares a modular architecture with SCOFF, but the modules have a fixed function and do not directly communicate with one another. This earlier work focused on language not images.

**Recurrent Independent Mechanisms (RIMs).** RIMs [Goyal et al., 2019] are a key inspiration for our work. RIMs are a modular neural architecture consisting of an ensemble of dynamical components which have sparse interactions through the bottleneck of attention. Each RIMs module has at its core an LSTM layer [Hochreiter and Schmidhuber, 1997]. A RIMs module is much like our object file. Both are meant to be dynamical entities with a time-evolving state. However, in contrast to files in SCOFF, RIMs modules operate according to fixed dynamics and each RIMs module is specialized for a particular computation. RIMs modules are thus not interchangeable.

**Relational RNN (RMC).** The RMC [Santoro et al., 2018] has a multi-head attention mechanism which allows it to share information between multiple memory locations. RMC is like Memory Networks in that dynamics are driven by a central controller: memory is used to condition the dynamics of an RNN.

**Neural Module Networks.** In Andreas et al. [2016], a neural network is composed dynamically from several neural modules, where each module is meant to perform a distinct function. Each module has a fixed function, unlike our files, and modules are applied one at a time, in contrast to our files, which can update and be used for prediction in parallel.

## 4 Experiments

We first explain how the SCOFF model is configured. Note that it is a drop-in replacement for a standard LSTM or GRU cell, conforming to the same input-output interface. Thus, integrating SCOFF is straightforward and only requires setting the number of object files and schemata.

### 4.1 Model setup

We use a one layered network, consisting of a set of files, and a set of schemata. The proposed architecture has 2 degrees of freedom: the number of object files and the number of schemata. For the supervised loss, the final state of the recurrent model is passed through a feed-forward network

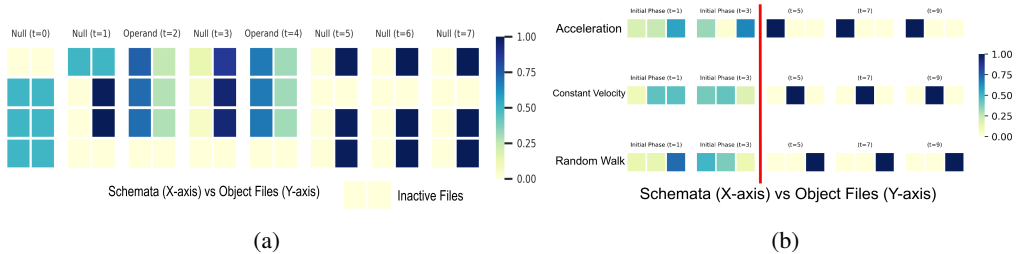


Figure 3: (a) Object Files ( $n_f = 4$ ) vs Schemata ( $n_s = 2$ ) activation for an example of length 8 of the adding task. "Null" refers to the elements other than the operands on which the addition is to be performed. The figure shows the affinity of each file to use a particular schemata. Each row corresponds to a particular file, and column represents a particular schemata (dark color shows high affinity of a file towards a particular schemata). As shown in the figure, the active files trigger Schema 1 when an operand is encountered, and Schema 2 when a "Null" element is encountered. (b) Here, we have a single object file, and that can follow three different dynamics. We found that our method is able to learn these 3 different modes once it's passed an initial phase of uncertainty.

Number of Values	LSTM	RIMS	SCOFF
2	0.8731	0.0007	0.0005
3	1.3017	0.0009	0.0007
4	1.6789	0.0014	0.0013
5	2.0334	0.0045	0.0030
8	4.8872	0.0555	0.0191
9	7.3730	0.1958	0.0379
10	11.3595	0.8904	0.0539

Table 1: **Adding Task:** Mean test set error on 200 length sequences with number of numbers to add varying among  $\{2, 3, 4, 5, 8, 9, 10\}$ . The models are trained to add a mixture of two and four numbers from sequences of length 50.

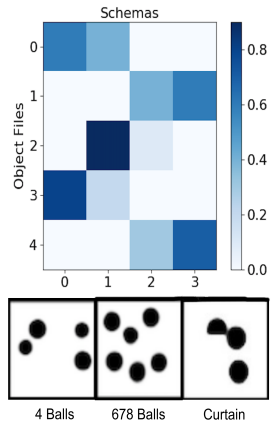


Figure 4: Object files and schema binding on RL task (top), Bouncing Balls Dataset (bottom).

before making a prediction. For video prediction experiments, the state of the concatenation is fed into the decoder, and it is then used for generating the image. Unless otherwise indicated we always (a) learn an embedding of size 600 at the output of an encoder, in an end-to-end fashion, for transforming per-time step inputs before feeding these encoded representations to the RNNs; (b) use Adam [Kingma and Ba, 2014] with a learning rate of 0.0001 and momentum of 0.9; and (c) set the number of object files and number of object files to select as  $n_f = 6$  and  $n_{sel} = 4$ , respectively. We include more experimental results and the code in the Supplementary Material, and we do plan to release the code. For more details please refer to the appendix section A.

**Baselines:** We compare the proposed method with *RMC*, a memory based relational recurrent model with attention between saved memory and hidden states [Santoro et al., 2018]. We also compare the proposed method to *Recurrent Independent Mechanisms (RIMs)*, a modular memory based on a single layered recurrent model with attention modulated input and communication between modules [Goyal et al., 2019].

## 4.2 Different schemata specializing over temporal patterns: Qualitative dynamics

### 4.2.1 Adding task

We analyzed the proposed method on the adding task. This is a standard task for investigating recurrent models [Hochreiter and Schmidhuber, 1997]. The input consists of two co-occurring sequences: 1)  $N$  numbers  $(a_0 \cdots a_{N-1})$  sampled independently from  $U[0, 1]$ , 2) an index  $i_0$  in the first half of the sequence, and an index  $i_1$  in the second half of the sequence together encoder as a one hot sequences. The target output is  $a_{i_0} + a_{i_1}$ . As shown in figure 3 (a), we can clearly observe the factorisation of procedural knowledge into two schemata effectively, one schema is triggered when an operand is encountered and the other when non-operand is encountered. For more details, we ask the reader to refer to appendix section B.

**Generalization Result:** For demonstrating the generalization capability of SCOFF, we consider a scenario where the models are trained to add a mixture of two and four numbers from sequences of length 50. They are evaluated on adding variable number (2-10) of numbers on 200 length sequences. As shown in Table 1, we note better generalization when using SCOFF. The dataset consists of 50,000 training sequences and 20,000 testing sequences for each different number of numbers to add. For more details about the hyperparameters, please refer to appendix section B.

### 4.2.2 Single object file and specialization over different schemata

To demonstrate that the proposed model is able to factorize different schemata, we consider the scenario, where there's only a single object file (i.e., single object), and that single object can follow different dynamics corresponding to different schemata. Specifically, the model is provided with a few frames depicting the single moving object, and the model is tasked with predicting it's trajectory. The object starts in random positions, and its dynamics are randomly selected from 3 alternatives (i.e., one that accelerates, one that moves at a constant velocity, and one that follows a random motion). In the context of SCOFF, this corresponds to a single object file and 3 different motion schemata. The main purpose of this very simple task is to provide an intuitive understanding how the proposed system SCOFF works. As shown in figure 3 (b), SCOFF is effective in factorising the knowledge of three different dynamics to three individual schemata. For more details, see Appendix C.

**Reinforcement Learning:** We demonstrate improved performance on a 2D multi-room gridworld and found that schemata clearly shift when the agent changes rooms or approaches a distinct object, such as a door or key. Disentanglement is shown in Figure 4 (top). We use the GotoObjMaze environment (i.e MiniGrid-GotoObjMaze-v0) from [Chevalier-Boisvert et al., 2018]. Here, the agent has to navigate to an object, the object may be in another room. We use exactly the same RL setup as in [Chevalier-Boisvert et al., 2018] except we extend the setup in BabyAI to only apply RGB images of the world rather than symbolic state representations, and hence making the task much more difficult. Hyper-parameters for this task are listed in Tab. 5.

In this environment, the agent is expected to navigate a 3x3 maze of 6x6 rooms, randomly interconnected by doors to find an object like "key". Here we use only one object file, but different number of schemas (4 in this example). If we look at the object files (vs) schemata, schemata 4 is being triggered when the "key" is in agent's view as shown in fig. 13. See Appendix D for details.

## 4.3 Exploring multiple object files and multiple schemata in the balls environment

We demonstrate that SCOFF improves results when it is necessary to have multiple object files for which some files share the same schema. We consider a bouncing balls environment (Figure 4) in which multiple balls move with billiard ball dynamics [Van Steenkiste et al., 2018]. The dataset consists of 50,000 training examples and 10,000 test examples showing  $\sim 50$  frames of either 4 solid balls bouncing in a confined square geometry (*4Balls*), 6-8 balls bouncing in a confined geometry (*678Balls*), 3 balls bouncing in a confined geometry with an occluded region (*Curtain*), or balls of different colors (*Colored 4Balls* and *Colored 678Balls*). The balls have distinct states (and hence distinct object files) but share underlying procedures (schema), which we aim to capture using SCOFF.

We trained baselines as well as proposed model for about 100 epochs. We use the same architecture for encoder as well as decoder as in [Van Steenkiste et al., 2018]. We found that SCOFF achieved dramatic improvements in successfully predicting rollouts relative to both LSTMs and RIMs (Figure 5 and Figure 6). We also found that improvements were achieved with a varying number of schemata  $n_s$  but that larger improvements were achieved when using a larger number of schemata, especially when

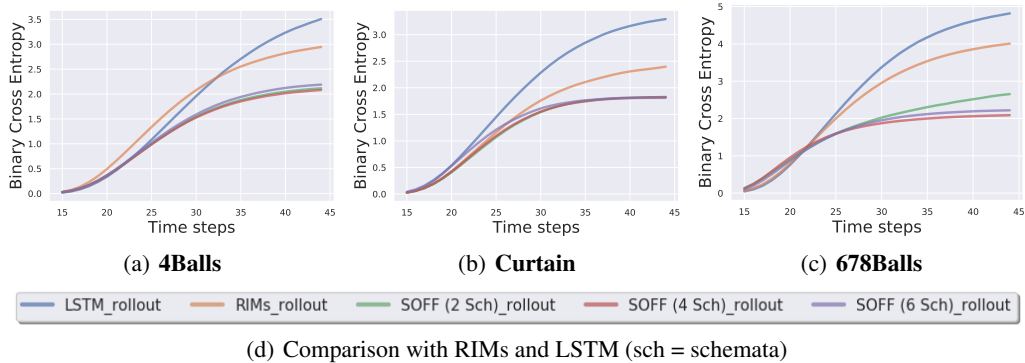


Figure 5: **Bouncing ball motion:** Prediction error comparison of SCOFF, LSTM, and RIMs. Given 10 frames of ground truth, the model predicts the rollout over the next 35 steps. SCOFF performs better than LSTM and RIMs in accurately predicting the dynamics. The advantage of SCOFF is amplified as the number of balls increases—(a) versus (c).

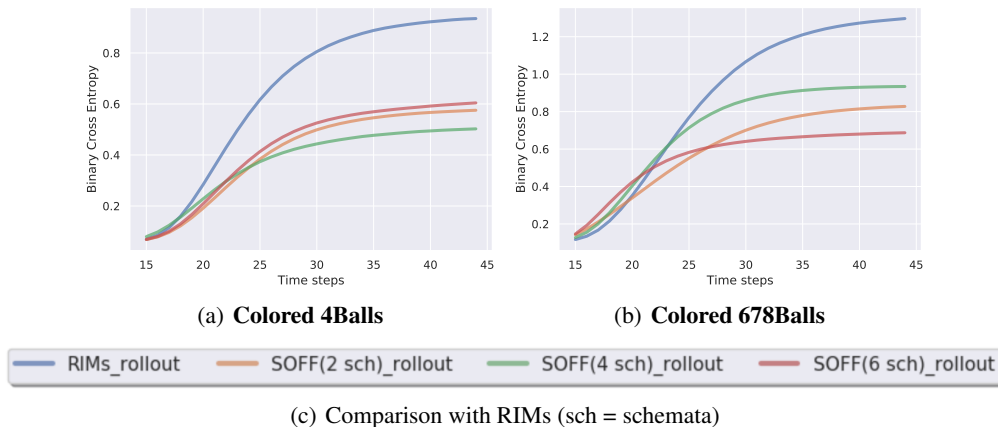


Figure 6: **Modelling Motion of Bouncing Balls:** Here, we have 4 balls or 678Balls. Each ball can have distinct color as compared to previous scenario. Here, we study the performance of SCOFF compared to RIMs baseline. The model receives the first 10 frames of ground truth as input and is tasked with predicting the next 35 time steps. During the rollout phase, the proposed model perform better than LSTMs, RIMs as well as RMC in accurately predicting the dynamics of the balls as reflected by the lower Cross Entropy (CE). Notice the substantially better performance of proposed method when testing on a higher number of objects (i.e, 6-8 objects).

modeling a larger number of balls. For more details regarding the predictions from the SCOFF and other baselines, please refer to appendix section C.

#### 4.4 Improved understanding of physical laws in a multi-object environment

One of our key motivations is to explore the importance of both declarative and procedural knowledge. One natural case study of this is the laws of physics (such as gravity, forces, etc.) which must be obeyed by all objects in the world, yet different objects have their own distinct states. For physical systems to be modeled correctly, this knowledge must be factorized correctly.

To test this more concretely, we used the Intuitive Physics Benchmark (Riochet et al. [2019]) in which balls roll behind a brick wall (so they are briefly occluded). The training data is constructed synthetically such that the examples are all physically realistic. Each test set consists of some realistic samples and some which follow obviously unrealistic physics. The types of unrealistic samples are as follows: balls disappearing behind the wall (O1 task), balls having their shape change for no reason (O2 task), or teleporting (O3 task). SCOFF improves performance on all these tasks (Table 2). We evaluate the proposed model on the “occlusion” subset of the task. For more details, see Appendix E.



Table 2: **Results on the IntPhys benchmark.** Relative classification error of unrealistic physical phenomenon for our model compared to Riochet et al. [2019], demonstrating benefits of our method in scenes with significant occlusions ("Occluded"). Lower is better. Averaged over 3 random seeds.

	Block O1 (Disappear)	Block O2 (Shape Change)	Block O3 (Teleport)
RMC	$0.43 \pm 0.05$	$0.39 \pm 0.03$	$0.46 \pm 0.02$
IntphysRiochet et al. [2019]	0.52	0.52	0.51
SCOFF (ours)	$0.29 \pm 0.02$	$0.35 \pm 0.05$	$0.42 \pm 0.02$

## 5 Conclusions

Understanding the visual world requires interpreting images in terms of distinct independent physical entities. These entities have persistent intrinsic properties, such as a color or velocity, and they have dynamics that transform the properties. We explored a mechanism that is able to factorize declarative knowledge (the properties) and procedural knowledge (the dynamics). Using attention, our SCOFF model learns this factorization into representations of entities—object files—and representations of how they transform over time—schemata. By applying the same schemata to multiple object files, SCOFF achieves systematicity of prediction, resulting in significantly improved generalization performance over state-of-the-art methods. It also addresses a fundamental issue in AI and cognitive science: the distinction between *types* and *tokens*. SCOFF is also interpretable, in that we can identify the binding between schemata and entity behavior. The factorization of declarative and procedural knowledge has broad applicability to a wide variety of challenging deep learning prediction tasks.

## 6 Acknowledgements

The authors acknowledge the important role played by their colleagues at Mila throughout the duration of this work. The authors would like to thank Danilo Jimenez Rezende and Rosemary Nan Ke for useful discussions. The authors are grateful to Sjoerd van Steenkiste, Nicolas Chapados, Pierre-André Noël for useful feedback. The authors are grateful to NSERC, CIFAR, Google, Samsung, Nuance, IBM, Canada Research Chairs, Canada Graduate Scholarship Program, Nvidia for funding, and Compute Canada for computing resources. We are very grateful to Google for giving Google Cloud credits used in this project.

## References

- Jacob Andreas, Marcus Rohrbach, Trevor Darrell, and Dan Klein. Neural module networks. In *Proceedings of the IEEE Conference on Computer Vision and Pattern Recognition*, pages 39–48, 2016.
- Maxime Chevalier-Boisvert, Dzmitry Bahdanau, Salem Lahlou, Lucas Willems, Chitwan Saharia, Thien Huu Nguyen, and Yoshua Bengio. Babyai: First steps towards grounded language learning with a human in the loop. *arXiv preprint arXiv:1810.08272*, 2018.
- Junyoung Chung, Caglar Gulcehre, KyungHyun Cho, and Yoshua Bengio. Empirical evaluation of gated recurrent neural networks on sequence modeling. *arXiv preprint arXiv:1412.3555*, 2014.
- Anirudh Goyal, Alex Lamb, Jordan Hoffmann, Shagun Sodhani, Sergey Levine, Yoshua Bengio, and Bernhard Schölkopf. Recurrent independent mechanisms. *arXiv preprint arXiv:1909.10893*, 2019.
- Alex Graves, Greg Wayne, Malcolm Reynolds, Tim Harley, Ivo Danihelka, Agnieszka Grabska-Barwińska, Sergio Gómez Colmenarejo, Edward Grefenstette, Tiago Ramalho, John Agapiou, et al. Hybrid computing using a neural network with dynamic external memory. *Nature*, 538(7626):471, 2016.
- Mikael Henaff, Jason Weston, Arthur Szlam, Antoine Bordes, and Yann LeCun. Tracking the world state with recurrent entity networks. *arXiv preprint arXiv:1612.03969*, 2016.
- Sepp Hochreiter and Jürgen Schmidhuber. Long short-term memory. *Neural computation*, 9(8): 1735–1780, 1997.

- Eric Jang, Shixiang Gu, and Ben Poole. Categorical reparameterization with gumbel-softmax. *arXiv preprint arXiv:1611.01144*, 2016.
- D. Kahneman, A. Treisman, and B. J. Gibbs. The reviewing of object files: object-specific integration of information. *Cognitive psychology*, 24(2):175–219, 1992.
- Diederik Kingma and Jimmy Ba. Adam: A method for stochastic optimization. *arXiv preprint arXiv:1412.6980*, 2014.
- Michael C Mozer and Sreerupa Das. A connectionist symbol manipulator that discovers the structure of context-free languages. In S. J. Hanson, J. D. Cowan, and C. L. Giles, editors, *Advances in Neural Information Processing Systems 5*, pages 863–870. Morgan-Kaufmann, 1993.
- Ronan Riochet, Mario Ynocente Castro, Mathieu Bernard, Adam Lerer, Rob Fergus, Véronique Izard, and Emmanuel Dupoux. Intphys: A benchmark for visual intuitive physics reasoning. 2019.
- Adam Santoro, Ryan Faulkner, David Raposo, Jack W. Rae, Mike Chrzanowski, Theophane Weber, Daan Wierstra, Oriol Vinyals, Razvan Pascanu, and Timothy P. Lillicrap. Relational recurrent neural networks. *CoRR*, abs/1806.01822, 2018. URL <http://arxiv.org/abs/1806.01822>.
- Sainbayar Sukhbaatar, arthur szlam, Jason Weston, and Rob Fergus. End-to-end memory networks. In C. Cortes, N. D. Lawrence, D. D. Lee, M. Sugiyama, and R. Garnett, editors, *Advances in Neural Information Processing Systems 28*, pages 2440–2448. Curran Associates, Inc., 2015. URL <http://papers.nips.cc/paper/5846-end-to-end-memory-networks.pdf>.
- Sjoerd Van Steenkiste, Michael Chang, Klaus Greff, and Jürgen Schmidhuber. Relational neural expectation maximization: Unsupervised discovery of objects and their interactions. *arXiv preprint arXiv:1802.10353*, 2018.

# Appendices

## A Implementation Details and Hyperparameters

The model setup consists of three main components: an encoder, the process of interaction between object files and schemata followed by a decoder.

**Resources Used:** It takes about 2 days to train the proposed model on bouncing ball task for 100 epochs on V100 (32G). We did not do any hyper-parameter search specific to a particular dataset (i.e 4Balls or 678Balls or Curtain Task). We ran the proposed model for different number of schemata (i.e 2/4/6). Similarly, it takes about 3 days to run for 20M steps for the Reinforcement learning task.

## B Adding Task

All the models are trained for 100 epochs with a learning rate of 0.001 using the Adam optimizer. We use 300 as the hidden dimension for both the LSTM baseline and the LSTM’s in RIMS, SCOFF. Table 3 lists the different hyperparameters used for training SCOFF.

Table 3: Hyperparameters for the adding generalization task

Parameter	Value
Number of object files ( $n_f$ )	5
Number of schemata ( $n_s$ )	2
Number of activated object files ( $n_{sel}$ )	2
Optimizer	Adam[Kingma and Ba, 2014]
learning rate	$1 \cdot 10^{-2}$
batch size	64
Inp keys	64
Inp Values	60
Inp Heads	4
Inp Dropout	0.1
Comm keys	32
Comm Values	32
Comm heads	4
Comm Dropout	0.1

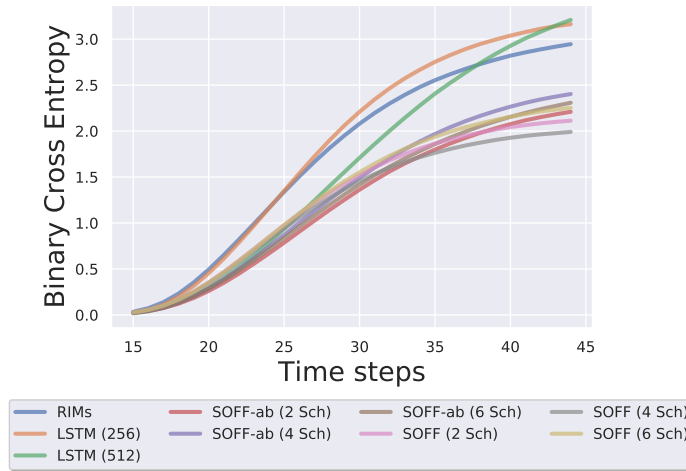
## C Bouncing Ball

The dataset consists of 50,000 training examples and 10,000 test examples showing  $\sim 50$  frames of either 4 solid balls bouncing in a confined square geometry (*4Balls*), 6-8 balls bouncing in a confined geometry (*678Balls*), 3 balls bouncing in a confined geometry with an occluded region (*Curtain*), or balls of different colors (*Colored 4Balls* and *Colored 678Balls*). The balls have distinct states (and hence distinct object files) but share underlying procedures (schema), which we aim to capture using SCOFF.

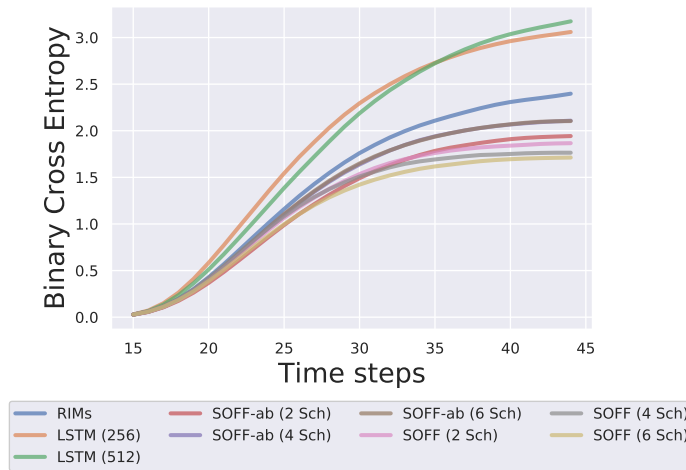
We trained baselines as well as proposed model for about 100 epochs. We use the same architecture for encoder as well as decoder as in [Van Steenkiste et al., 2018]. We also provide an ablation when all the object files are activated i.e.  $n_{sel} = n_f$ , and denote the corresponding model as SCOFF-ab. The prediction error comparison of all the models are given in the Figure 7. We also provide the rollouts predicted by the models in the Figures 8, 10, 9, 11, 12. As shown in Figure 7, SCOFF models that activate subset of object files perform better than SCOFF-ab.

## D BabyAI: Reinforcement Learning

We use the GotoObjMaze environment (i.e MiniGrid-GotoObjMaze-v0) from [Chevalier-Boisvert et al., 2018]. Here, the agent has to navigate to an object, the object may be in another room. We



(a) **4Balls**



(b) **Curtain**

Figure 7: Prediction error comparison of SCOFF, SCOFF-ab, RIMs and LSTM. The model receives the first 10 frames of ground truth are given as the input and is tasked with predicting the next 35 time steps. We also provide an ablation when all the object files are activated i.e.  $n_{\text{sel}} = n_f$ , and denote the corresponding model as SCOFF-ab. As figure shows, SCOFF performs slightly better as compared to SCOFF-ab.

Table 4: Hyperparameters for the bouncing balls task

Parameter	Value
Number of object files ( $n_f$ )	6
Number of schemata ( $n_s$ )	2/4/6
Number of activated object files ( $n_{sel}$ )	4
Size of Hidden state of object file	85
Optimizer	Adam[Kingma and Ba, 2014]
learning rate	$1 \cdot 10^{-4}$
batch size	64
Inp keys	64
Inp Values	85
Inp Heads	1
Inp Dropout	0.1
Comm keys	32
Comm Values	32
Comm heads	4
Comm Dropout	0.1

use exactly the same RL setup as in [Chevalier-Boisvert et al., 2018] except we extend the setup in BabyAI to only apply RGB images of the world rather than symbolic state representations, and hence making the task much more difficult. Hyper-parameters for this task are listed in Tab. 5.

In this environment, the agent is expected to navigate a 3x3 maze of 6x6 rooms, randomly interconnected by doors to find an object like "key". Here we use only one object file, but different number of schemas (4 in this example). If we look at the object files (vs) schemata, schemata 4 is being triggered when the "key" is in agent's view as shown in fig. 13.

Table 5: Hyperparameters for BabyAI

Parameter	Value
Number of object files ( $n_f$ )	1
Number of schemata ( $n_s$ )	2/4/6
Size of Hidden state of object file	510
Number of activated object files ( $n_{sel}$ )	1
Optimizer	Adam[Kingma and Ba, 2014]
Learning rate	$3 \cdot 10^{-4}$
Inp keys	64
Inp Values	85
Inp Heads	4
Inp Dropout	0.1
Comm keys	16
Comm Values	32
Comm heads	4
Comm Dropout	0.1

## E Intuitive Physics

We use the similar training setup as [Riochet et al., 2019]. Hyper-parameters related to the proposed method are listed in Tab. 6.

Table 6: Hyperparameters for IntPhys benchmark

Parameter	Value
Number of object files ( $n_f$ )	6
Number of schemata ( $n_s$ )	4/6
Number of activated object files ( $n_{sel}$ )	4
Optimizer	Adam[Kingma and Ba, 2014]
learning rate	$3 \cdot 10^{-4}$
batch size	64
Inp keys	64
Inp Values	85
Inp Heads	4
Inp Dropout	0.1
Comm keys	32
Comm Values	32
Comm heads	4
Comm Dropout	0.1

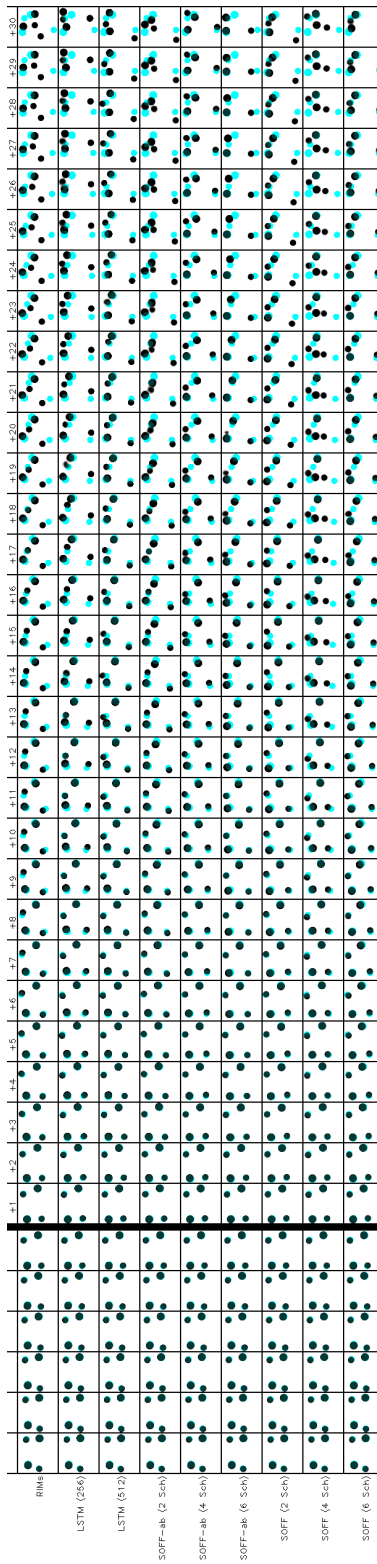


Figure 8: **Rollout for 4Balls.** In all cases, the first 10 frames of ground truth are fed in (last 6 shown) and then the system is rolled out for the next 30 time steps. In the predictions, the transparent blue shows the ground truth, overlaid to help guide the eye.

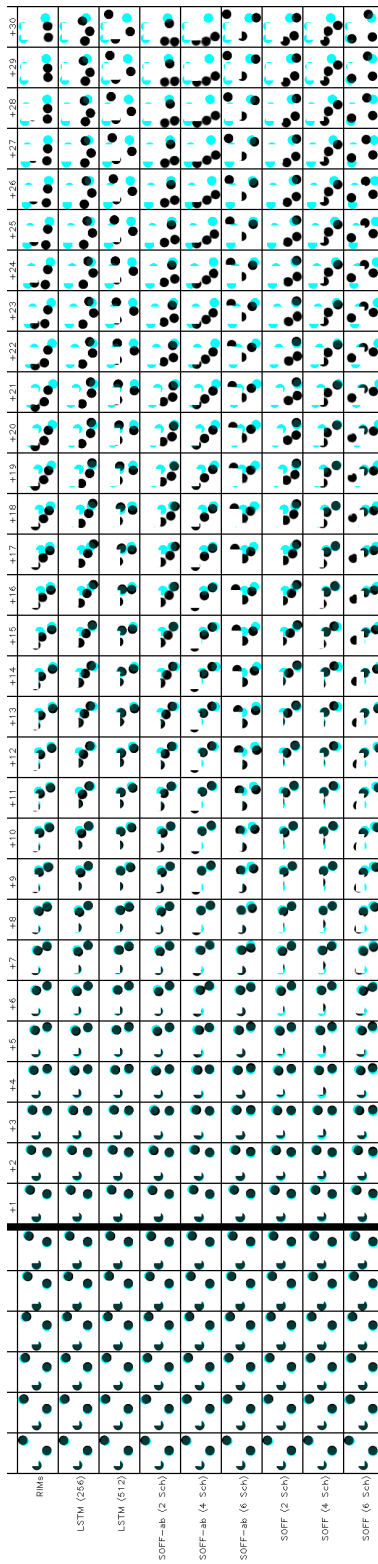


Figure 9: **Rollout for Curtain.** In all cases, the first 10 frames of ground truth are fed in (last 6 shown) and then the system is rolled out for the next 30 time steps. In the predictions, the transparent blue shows the ground truth, overlaid to help guide the eye.



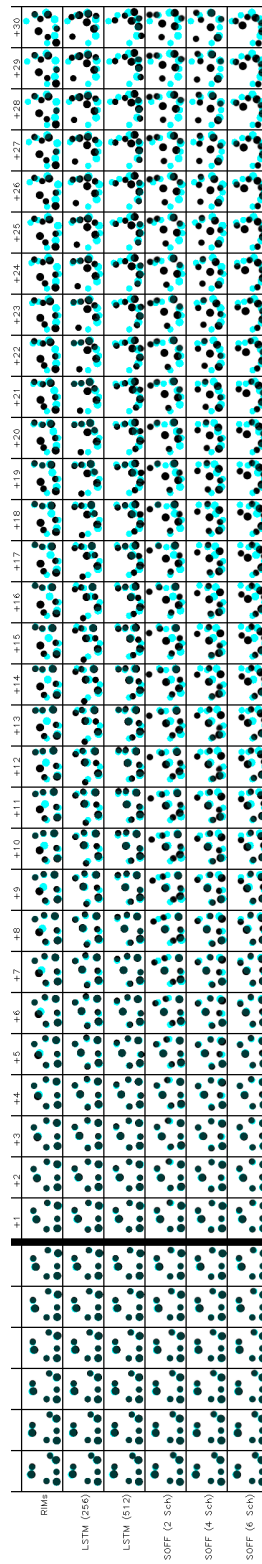


Figure 10: **Rollout for 678Balls**. In all cases, the first 10 frames of ground truth are fed in (last 6 shown) and then the system is rolled out for the next 30 time steps. In the predictions, the transparent blue shows the ground truth, overlaid to help guide the eye.

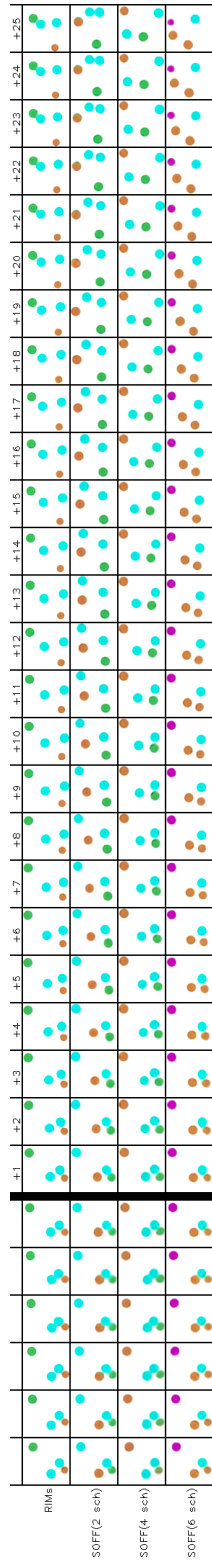


Figure 11: **Rollout for Colored 4Balls.** In all cases, the first 10 frames of ground truth are fed in (last 6 shown) and then the system is rolled out for the next 25 time steps.

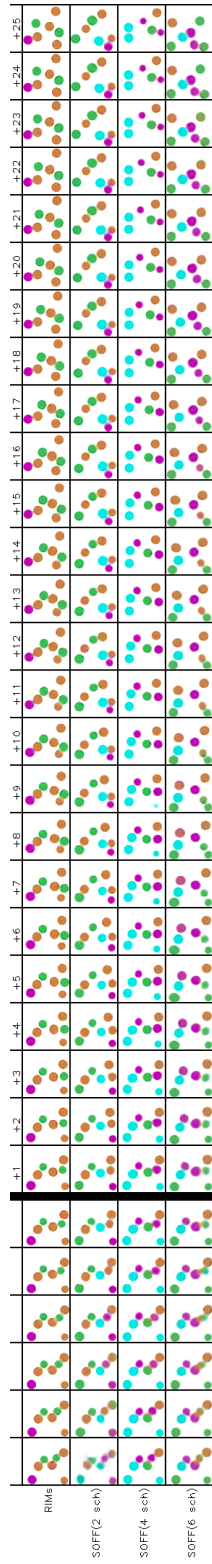
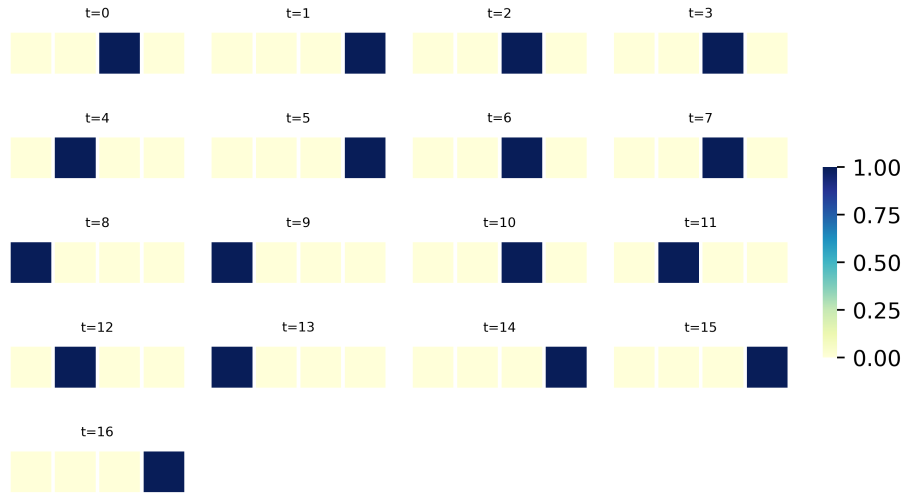
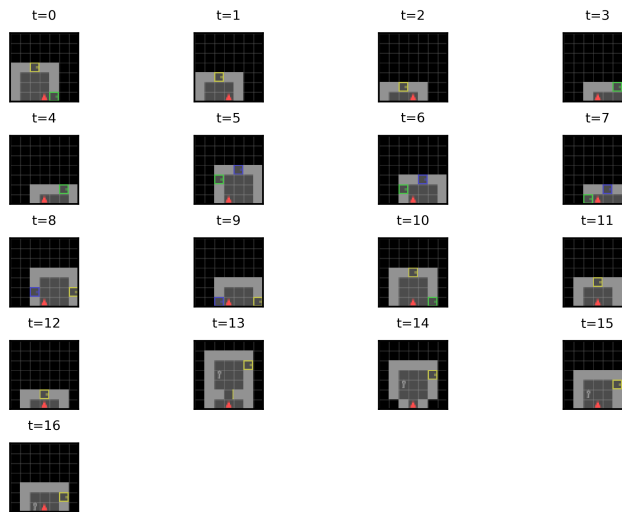


Figure 12: **Rollout for Colored 678Balls.** In all cases, the first 10 frames of ground truth are fed in (last 6 shown) and then the system is rolled out for the next 25 time steps.



(a) Object Files ( $n_f = 1$ ) (vs) Schemata ( $n_s = 4$ ) Activation



(b) Agent view in the environment

Figure 13: **BabyAI-GotoObjMaze Trajectory** In this environment, the agent is expected to navigate a 3x3 maze of 6x6 rooms, randomly inter-connected by doors to find an object like "key". Here we use only one object file, but different number of schemata (4 in this example). If we look at the object files (vs) schemata affinity, schema 1 is activated while close to or opening doors while schema 4 is triggered when the "key" is in the agent's view.